Available online at www.sciencedirect.com
SCIENCE DIRECT®
PHYTOCHEMISTRY
Phytochemistry 65 (2004) 1937–1954
www.elsevier.com/locate/phytochem

Fresh organically grown ginger (*Zingiber officinale*): composition and effects on LPS-induced PGE_2 production

Shivanand D. Jolad [a], R. Clark Lantz [a,c], Aniko M. Solyom [a], Guan Jie Chen [a,c], Robert B. Bates [d], Barbara N. Timmermann [a,b,*]

[a] *Arizona Center for Phytomedicine Research, College of Pharmacy, University of Arizona, Tucson, AZ 85721, USA*
[b] *Department of Pharmacology and Toxicology, College of Pharmacy, University of Arizona, Tucson, AZ 85721, USA*
[c] *Department of Cell Biology and Anatomy, College of Medicine, University of Arizona, Tucson, AZ 85724, USA*
[d] *Department of Chemistry, University of Arizona, Tucson, AZ 85721, USA*

Received 28 January 2004; received in revised form 13 April 2004
Available online 20 July 2004

Abstract

Gas chromatography in conjunction with mass spectrometry, a technique previously employed to analyze non-volatile pungent components of ginger extracts modified to trimethylsilyl derivatives, was applied successfully for the first time to analyze unmodified partially purified fractions from the dichloromethane extracts of organically grown samples of fresh Chinese white and Japanese yellow varieties of ginger, *Zingiber officinale* Roscoe (Zingiberaceae). This analysis resulted in the detection of 20 hitherto unknown natural products and 31 compounds previously reported as ginger constituents. These include paradols, dihydroparadols, gingerols, acetyl derivatives of gingerols, shogaols, 3-dihydroshogaols, gingerdiols, mono- and diacetyl derivatives of gingerdiols, 1-dehydrogingerdiones, diarylheptanoids, and methyl ether derivatives of some of these compounds. The thermal degradation of gingerols to gingerone, shogaols, and related compounds was demonstrated. The major constituent in the two varieties was [6]-gingerol, a chemical marker for *Z. officinale*. Mass spectral fragmentation patterns for all the compounds are described and interpreted. Anti-inflammatory activities of silica gel chromatography fractions were tested using an in vitro PGE_2 assay. Most of the fractions containing gingerols and/or gingerol derivatives showed excellent inhibition of LPS-induced PGE_2 production.

Keywords: *Zingiber officinale*; Zingiberaceae; Ginger; Rhizomes; Ginger derivatives

1. Introduction

Chronic obstructive pulmonary disease, asthma and rheumatoid arthritis are associated with chronic inflammation. Treatment of these diseases with therapeutic pharmaceuticals has met with some success. In addition, patients suffering from diseases with associated chronic inflammation are turning to alternatives for relief of their symptoms or as prophylactic treatments. These alternatives include dietary supplements that have been purported to have anti-inflammatory actions. However, the efficacy and the potency of these supplements have not been studied in great detail nor have the active compounds been identified.

Ginger [*Zingiber officinale* Roscoe (Zingiberaceae)] and supplements derived from ginger have received attention for the treatment of chronic inflammation. Administration of ginger has resulted in decreased symptoms of rheumatoid arthritis (Srivastava and Mustafa, 1992) and gingerol (a component of ginger) has been reported to have anti-inflammatory actions, which include suppression of both cyclooxygenase and lipooxygenase metabolites of arachidonic acid (Kiuchi et al., 1992; Srivas, 1984; Tjendraputra et al., 2001).

Previous quantitative analyses of ginger have shown that gingerols, a family of homologous compounds differentiated by the number of carbon atoms in their

* Corresponding author. Tel.: +1-520-626-2481; fax: +1-520-626-2515.
E-mail address: btimmer@pharmacy.arizona.edu (B.N. Timmermann).

0031-9422/$ - see front matter © 2004 Elsevier Ltd. All rights reserved.
doi:10.1016/j.phytochem.2004.06.008

side chain, are the major pungent constituents, with [6]-gingerol [5-hydroxy-1-(4′-hydroxy-3′-methoxyphenyl) decan-3-one] being the most abundant (Govindarajan, 1982). Another homologous series which also accounts for the pungency of ginger is the shogaol family, the dehydrated form of the gingerols, resulting from the elimination of the OH group at C-5 with the formation of a double bond between C-4 and C-5. The shogaols are known to occur naturally and also are formed chemically from the corresponding gingerols in pH 2.5–7.2 media and during thermal processing, long-term storage and chromatography over silica gel and alumina (Connell and Sutherland, 1969; Mustafa et al., 1993). The distinct aroma of fresh ginger comes from the volatile oils, the second major group of components of ginger. The presence of these volatile oils, which were not investigated in this study, makes the separation of minor non-volatile pungent components difficult.

Various analytical techniques employing chromatographic methods such as GLC and GC in conjunction with mass spectroscopy have been used to analyze pungent components in ginger by modifying the ginger extract and/or partially purified fractions to their trimethylsilyl (TMS) derivatives with a view to improve their volatility, stability and separation (Masada et al., 1973; Clark et al., 1977; Harvey, 1981; Masada et al., 1974). More recently, He et al. (1998) described the analysis of ginger constituents by the combination of high pressure liquid chromatography with UV photodiode array detection and electrospray mass spectrometry (HPLC–UV–ESMS).

We have separated organic extracts from Chinese white and Japanese yellow ginger rhizomes by silica gel chromatography, finding many fractions which have in vitro anti-inflammatory activity. GC–MS analysis of the underivatized active fractions provided excellent resolution of the sixty three (**1**–**63**) components, most of which could be identified from their mass spectral fragmentations. These included 31 previously reported ginger constituents, 20 new natural products, and 12 artifacts produced by thermal degradation of the gingerols. Some of the active fractions contained little or no gingerols, but these contained gingerol derivatives.

2. Results and discussion

Only those CC fractions that demonstrated anti-inflammatory activity in the PGE_2 assay were subjected to GC–MS analysis to detect and identify the constituents present in them. The yields of the CC fractions from GF2-00 and GF3-00, their PGE_2 assay profile and the broad spectrum of compounds detected are summarized in Table 1. Individual compounds (**1**–**56**) identified are listed in Table 2 together with their MS (molecular ion and base peaks) characteristics, while thermal degradation products (**57**–**63**) with similar attributes are listed separately in Table 3. The results of the quantitative analyses of [6]-, [8]- and [10]-gingerols and [6]-shogaol in the CH_2Cl_2 extracts of white (GF2-00) and yellow (GF3-00) gingers are summarized in Table 4. These results show that the three gingerols were predominant in both varieties but their presence in the yellow variety was at a higher concentration (47%) than in the white variety (36%). The most abundant constituent was [6]-gingerol (**10**), representing nearly 34% and 28% in the yellow and white varieties, respectively, followed by [10]- and [8]-gingerols (**13** and **12**). The presence of [6]-shogaol (**17**) at a meager level of 0.35% in both varieties suggests that it could be either an artifact derived from [6]-gingerol (**10**) via dehydration during processing or a naturally occurring minor constituent.

The efficacy of the methodology employed in this investigation is illustrated with GC chromatograms of three CC fractions in Fig. 1. Peaks with retention times $Rt < 20$ min were not studied except for the compounds in which the peak at m/z 137 was seen as the base peak (or shifted upward by 14 mass units to m/z 151 or downward by 30 mass units to m/z 107), the most distinctive peak associated with the 4′-hydroxy-3′-methoxybenzyl cation ($C_8H_9O_2$ by HRMS) seen in the mass spectra of almost all compounds identified in this investigation. Compounds listed in Table 3 (**57**–**63**) were detected in the region below $Rt < 20$ min. Other compounds in this region appeared to be mostly $C_{15}H_{22}$ and $C_{15}H_{24}$ sesquiterpenes and hydroxylated sesquiterpenes based on the observed molecular ion ($[M]^+$) and subsidiary peaks (Yu et al., 1998; Sharma et al., 2002). All other compounds listed in Table 2 (**1**–**56**) were detected in the region $Rt > 20$ min.

All compounds listed in Table 2 have the 4′-hydroxy-3′-methoxyphenyl moiety (two in **48** and **49**) and a substituent at C-3 except **46** which lacks the methoxy group in the phenyl ring. The OH group in the phenyl ring is methylated in methyl ether derivatives. Except for paradols (**1**–**8**), all compounds have a substituent at C-5 which is replaced by a double bond between C-4/C-5 in shogaols (**16**–**22**) and in **46** and **48**. Dehydrogingerdiones (**28**–**31** and **50**) contain an additional double bond between C-1 and C-2.

2.1. Fragmentations

The main fragmentation routes in the mass spectra of compounds listed in Table 2 are directed by the substituents at C-1, C-3 and C-5, thus offering a means for identification of their nature and location. This together with the size of the molecule from their molecular ion peak and the occurrence of a base peak at m/z 137 (the benzylic cleavage product associated with the 4′-hydroxy-3′-methoxybenzyl cation), which is a feature of the mass spectra of all compounds except in dehydrogingerdiones, showed the chain length. The upward

Table 1
Summary of extraction and column chromatography fractionation profile of white and yellow ginger varieties: yields, activity in inhibiting in vitro PGE_2 production and the general class of compounds detected by GC–MS in the active fractions

White ginger (**GF2**)					Yellow ginger (**GF3**)				
Extract/fraction	Yield (g)	Cytotoxic dose (μg/ml)	PGE_2IC_{50} (μg/ml)	Components	Extract/fraction	Yield (g)	Cytotoxic dose (μg/ml)	PGE_2IC_{50} (μg/ml)	Components
GF2-ZZ	2.22	–	3.47	–	GF3-ZZ	1.72	–	–	
GF2-00	16.56	10	0.051	Original	GF3-00	17.90	50	0.072	Original
GF2-01	1.590	5	0.082	Sesquiterpenes and non-gingerols	GF3-01	1.108	1	9.9	[a]
GF2-02	0.688	–	0.336		GF3-02	0.396	–	5.07	[a]
GF2-03	0.197	50	0.066		GF3-03	0.161	10	0.320	[a]
GF2-04	0.092	50	0.06		GF3-04	0.390	–	40.87	[a]
GF2-05	0.138	–	0.076	Paradols	GF3-05	0.663	–	0.068	Paradols
GF2-06	0.566	–	0.056		GF3-06	1.200	50	0.064	
GF2-07	0.972	50	0.053		GF3-07	0.127	–	0.093	Shogaols and dehydrogingerdiones
GF2-08	0.706	50	0.054	Shogaols and dehydrogingerdiones	GF3-08	0.596	50	0.082	
GF2-09	0.099	50	0.054		GF3-09	0.331	–	0.074	Acetyl derivatives of gingerols
GF2-10	0.351	50	0.054		GF3-10	0.310	10	0.071	
GF2-11	0.247	50	0.053	Acetyl derivatives of gingerols	GF3-11	0.727	50	0.068	Gingerols
GF2-12	0.291	50	0.054		GF3-12	3.172	50	0.068	
GF2-13	1.133	50	0.053	Gingerols	GF3-13	2.077	–	0.068	
GF2-14	1.639	–	0.07		GF3-14	0.592	–	0.064	
GF2-15	1.500	–	0.066		GF3-15	0.235	10	0.065	
GF2-16	0.345	50	0.069		GF3-16	1.141	50	0.069	Gingerdiols
GF2-17	0.307	50	0.079		GF3-17	1.186	50	0.374	[a]
GF2-18	1.293	–	0.068	Gingerdiols	GF3-18	3.180	–	9	[a]
GF2-19	1.067	50	0.978	[a]					
GF2-20	3.280	50	9.82	[a]					

[a] Not subjected to GC–MS analysis.

Table 2
Compounds identified by GC–MS in the column chromatographic fractions of fresh white (**GF2**) and yellow (**GF3**) ginger

Structure	*Cpd*	*n*	R	M^+	Base	*Name*
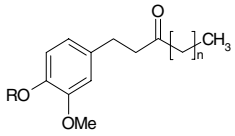	**1**	6	H	278	137	[6]-Paradol
	2	7	H	292	137	[7]-Paradol
	3	8	H	306	137	[8]-Paradol
	4	9	H	320	137	[9]-Paradol
	5	10	H	334	137	[10]-Paradol
	6[a]	11	H	348	137	[11]-Paradol
	7[a]	13	H	376	137	[13]-Paradol
	8[a,d]	6	Me	292	151	Methyl [6]-paradol
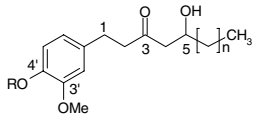	**9**	2	H	266	137	[4]-Gingerol
	10	4	H	294	137	[6]-Gingerol
	11[b]	5	H	308	137	[7]-Gingerol
	12	6	H	322	137	[8]-Gingerol
	13	8	H	350	137	[10]-Gingerol
	14[c]	2	Me	280	151	Methyl [4]-gingerol
	15	4	Me	308	151	Methyl [6]-gingerol
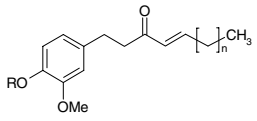	**16**	2	H	248	137	[4]-Shogaol
	17	4	H	276	137	[6]-Shogaol
	18	6	H	304	137	[8]-Shogaol
	19	8	H	332	137	[10]-Shogaol
	20	10	H	360	137	[12]-Shogaol
	21	4	Me	290	151	Methyl [6]-shogaol
	22	6	Me	318	151	Methyl [8]-shogaol
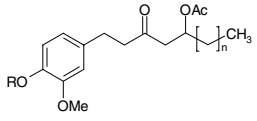	**23**[a]	2	H	308	137	Acetoxy-[4]-gingerol
	24	4	H	336	137	Acetoxy-[6]-gingerol
	25[a,b]	6	H	364	137	Acetoxy-[8]-gingerol
	26[a,b]	8	H	392	137	Acetoxy-[10]-gingerol
	27	4	Me	350	151	Methyl acetoxy-[6]-gingerol
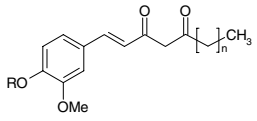	**28**[a]	1	H	248	145	1-Dehydro-[3]-gingerdione
	29	4	H	290	177	1-Dehydro-[6]-gingerdione
	30	6	H	318	177	1-Dehydro-[8]-gingerdione
	31	8	H	346	177	1-Dehydro-[10]-gingerdione
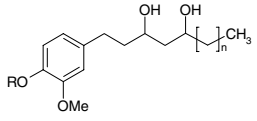	**32**	2	H	268	137	[4]-Gingerdiol
	33	4	H	296	137	[6]-Gingerdiol
	34[b]	6	H	324	137	[8]-Gingerdiol
	35	8	H	352	137	[10]-Gingerdiol
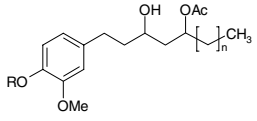	**36**[a]	2	H	310	137	5-Acetoxy-[4]-gingerdiol
	37	4	H	338	137	5-Acetoxy-[6]-gingerdiol
	38[a]	5	H	352	137	5-Acetoxy-[7]-gingerdiol
	39[a]	2	Me	324	151	Methyl 5-acetoxy-[4]-gingerdiol
	40[a]	4	Me	352	151	Methyl 5-acetoxy-[6]-gingerdiol
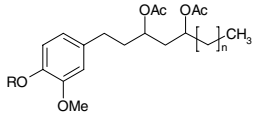	**41**	2	H	352	137	Diacetoxy-[4]-gingerdiol
	42	4	H	380	137	Diacetoxy-[6]-gingerdiol
	43[a]	2	Me	366	137	Methyl diacetoxy-[4]-gingerdiol
	44	4	Me	394	151	Methyl diacetoxy-[6]-gingerdiol
	45[a]	8	Me	460	330	Methyl diacetoxy-[10]-gingerdiol
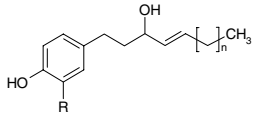	**46**[a,b]	4	–	248	107	3-Dihydro-[6]-demethoxyshogaol
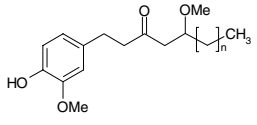	**47**[a]	4	H	308	137	5-Methoxy-[6]-gingerol

Table 2 (*continued*)

Structure	*Cpd*	*n*	R	M^+	Base	*Name*
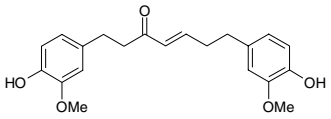	**48**	–	–	356	137	1,7-*bis*-(4′-Hydroxy-3′-methoxy-phenyl)-4-heptene-3-one
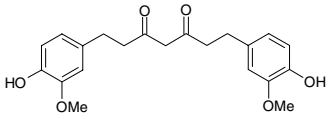	**49**[a,d]	–	–	372	137	1,7-*bis*-(4′-Hydroxy-3′-methoxy-phenyl)-3,5-heptadione
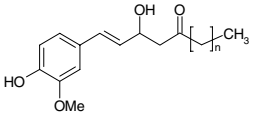	**50**[a,b]	8	–	348	177	1-Dehydro-3-dihydro-[10]-ginger-dione
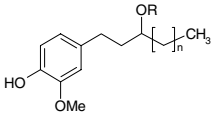	**51**[a,d]	6	H	280	137/138	6-Dihydroparadol
	52[a]	6	Ac	322	131	Acetoxy-6-dihydroparadol
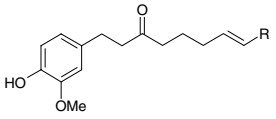	**53**	–	H	248	137	1-(4′-Hydroxy-3′-methoxyphe-nyl)-7-octen-3-one
	54	–	CH_2Me	276	137	1-(4′-Hydroxy-3′-methoxyphe-nyl)-7-decen-3-one
	55	–	$(CH_2)_3Me$	304	137	1-(4′-Hydroxy-3′-methoxyphe-nyl)-7-dodecen-3-one
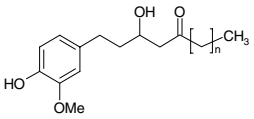	**56**[a,c]	2	–	266	137	[4]-Isogingerol

[a] Not previously reported from ginger.
[b] Not detected in white ginger.
[c] Not detected in yellow ginger.
[d] Reported as a synthetic product.

Table 3
Thermal degradation products detected by GC–MS

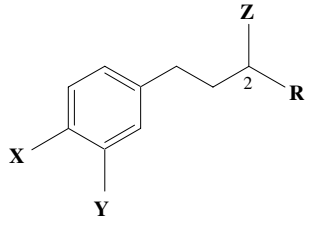

Cpd	X	Y	Z	R	$[M]^+$	Base	Name
57	OH	H	2-keto	Me	164	107	4-(4-Hydroxyphenyl)-2-butanone
58	OH	OMe	2-keto	H	180	137	4-Hydroxy-3-methoxybenzenepropanal
59	OMe	OMe	2-keto	H	194	151	3,4-Dimethoxybenzenepropanal
60	OH	OMe	2-keto	Me	194	137	Zingerone
61	OMe	OMe	2-keto	Me	208	151	Zingerone methyl ether
62	OH	OMe	OH	Me	196	137	Gingerol
63	OH	OMe	OMe	Me	210	137	Zingerol 2-methyl ether

Table 4
Summary of quantification of [6]-, [8]- and [10]-gingerols (**10**, **12** and **13**) and [6]-shogaol (**17**) in white (GF2-00) and yellow (GF3-00) ginger extracts

Sample name/ID	Sample composition (%)			
	[6]-Gingerol (**10**)	[8]-Gingerol (**12**)	[10]-Gingerol (**13**)	[6]-Shogaol (**17**)
White ginger ext (GF2-00)	27.56 ± 0.04	3.20 ± 0.04	5.38 ± 0.00	0.36 ± 0.02
Yellow ginger ext (GF3-00)	33.96 ± 0.17	4.64 ± 0.10	7.91 ± 0.19	0.35 ± 0.02

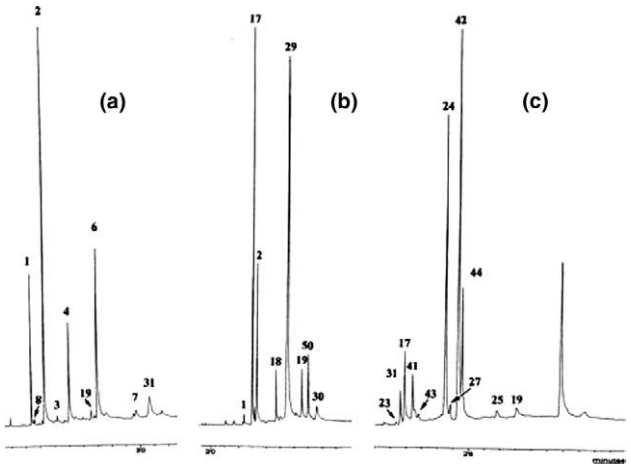

Fig. 1. GC chromatograms of fractions GF3-13F06 (a), GF3-13F08 (b) and GF3-13F10 (c), showing the resolution of peaks denoted by compound numbers listed in Table 2.

shift of the base peak from m/z 137 to 151 in the methyl ether derivatives and a nearly identical breakdown pattern with the appropriate shift of the molecular ion peak in the mass spectra of homologs further facilitated their identification.

Each compound was identified based on its characteristic fragmentation pattern, $[M]^+$ peak homology, subsidiary peaks derived from $[M]^+$, by comparison with the spectra of homologs and with published data as well as from the peak shifts in the spectra of naturally occurring derivatives present in the fractions. Gingerol, shogaol and paradol homologs were identified by comparison of their spectra with those of [6]-gingerol (**10**), [6]-shogaol (**17**) and [6]-paradol (**1**), respectively. The 5-acetyl derivatives of gingerols, which produced intense M-HOAc ions corresponding to M-H_2O ions in their parent compounds, fully supported the designated structures. The isolation of pure 1-dehydro-[6]-gingerdione (**29**) and its unique GC–MS fragmentation pattern allowed its use as a model from which to identify its homologs and related compounds. The diols were recognized from their two successive dehydration peaks from $[M]^+$, $[M]^+$ peak homology and the high intensity auxiliary peaks [(M-HOAc and M-(2HOAc)] appropriately shifted in the spectra of their naturally occurring mono- and diacetyl derivatives, respectively. Diarylheptanoids exhibited pairs of diagnostic peaks adding up to the *Mr* suggesting the presence of two 4′-hydroxy-3′-methoxybenzyl moieties. Methyl ether derivatives were clearly recognized, even in the presence of peaks associated with their parent compounds, from the diagnostic peaks appropriately shifted to higher m/z values by 14 mass units.

2.2. Gingerols (*9–15*)

[6]-Gingerol (**10**), the major constituent in the dichloromethane extracts of white (GF2-00) and yellow (GF3-00) fresh ginger, and its [8]- (**12**) and [10]- (**13**) homologs were identified by HPLC comparison with reference standards (Fig. 2). In the GC–MS, [10]-gingerol (**13**) was not detected but [4]- (**9**), [6]- (**10**), and [8]- (**12**) homologs in addition to the methylated derivatives

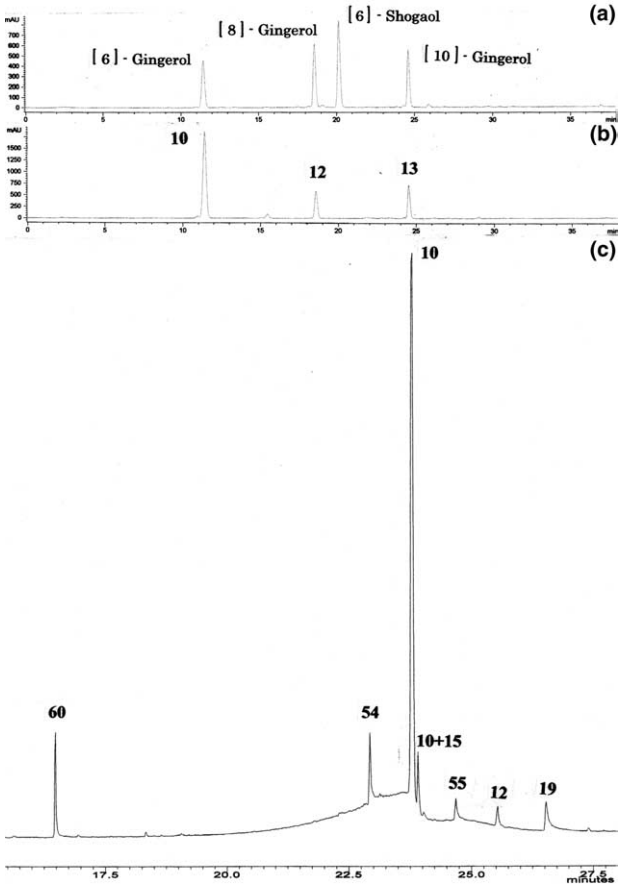

Fig. 2. (a) HPLC chromatogram of mixed reference standards (detection = 210 nm). (b) HPLC chromatogram of CC fraction GF3-F12. (c) GC chromatogram of CC fraction GF3-F12 showing thermal degradation products of gingerols. Peaks in (b) and (c) are identified by compound numbers listed in Table 2.

of [4]- (**14**) and [6]- (**15**) gingerols were identified. Their GC–MS spectra were very informative, exhibiting $[M]^+$ peak homology at m/z 266 (in **9**), 294 (in **10**) and 322 (in **12**) with appreciable intensity. The most distinctive peak with high abundance in these spectra, besides the base peak at m/z 137 associated with the 4′-hydroxy-3′-methoxybenzyl grouping, was at m/z 194, a product of McLafferty rearrangement (MLR). Another notable feature was a peak at m/z 205, resulting from the cleavage of the C-5/C-6 bond in the dehydrated (M-H_2O) ions at m/z 248 (in **9**), 276 (in **10**) and 304 (in **12**), same as the molecular ion peaks of [4]- (**16**), [6]- (**17**) and [8]- (**18**) shogaols, respectively. This key fragment at m/z 205 stands out in the GC–MS spectra of all [*n*]-shogaols (**16–22**) detected in this study. The GC–MS spectrum of [6]-gingerol (**10**), reproduced in Fig. 3, serves as an example and the geneses of major fragment ions are rationalized in Scheme 1.

The thermal degradation and dehydration of compounds containing β-hydroxyketone groupings, e.g. the [*n*]-gingerols, to aliphatic aldehydes and zingerones and to the corresponding [*n*]-shogaols under gas chromatographic conditions has long been noted (Connell and Sutherland, 1969; Connell and McLachian, 1972). To further test the validity of this phenomenon under our GC–MS conditions, a fraction (GF3-12) that contained a mixture of [6]- (**10**), [8]- (**12**) and [10]- (**13**) gingerols with no trace of shogaols as judged by HPLC (Fig. 2) was subjected to GC–MS. The chromatogram exhibited peaks representing [6]- (**10**) and [8]- (**12**) gingerols, and [10]-shogaol (**19**), zingerone (**60**) and traces of **58** and **61** but no peak corresponding to [10]-gingerol (**13**) was

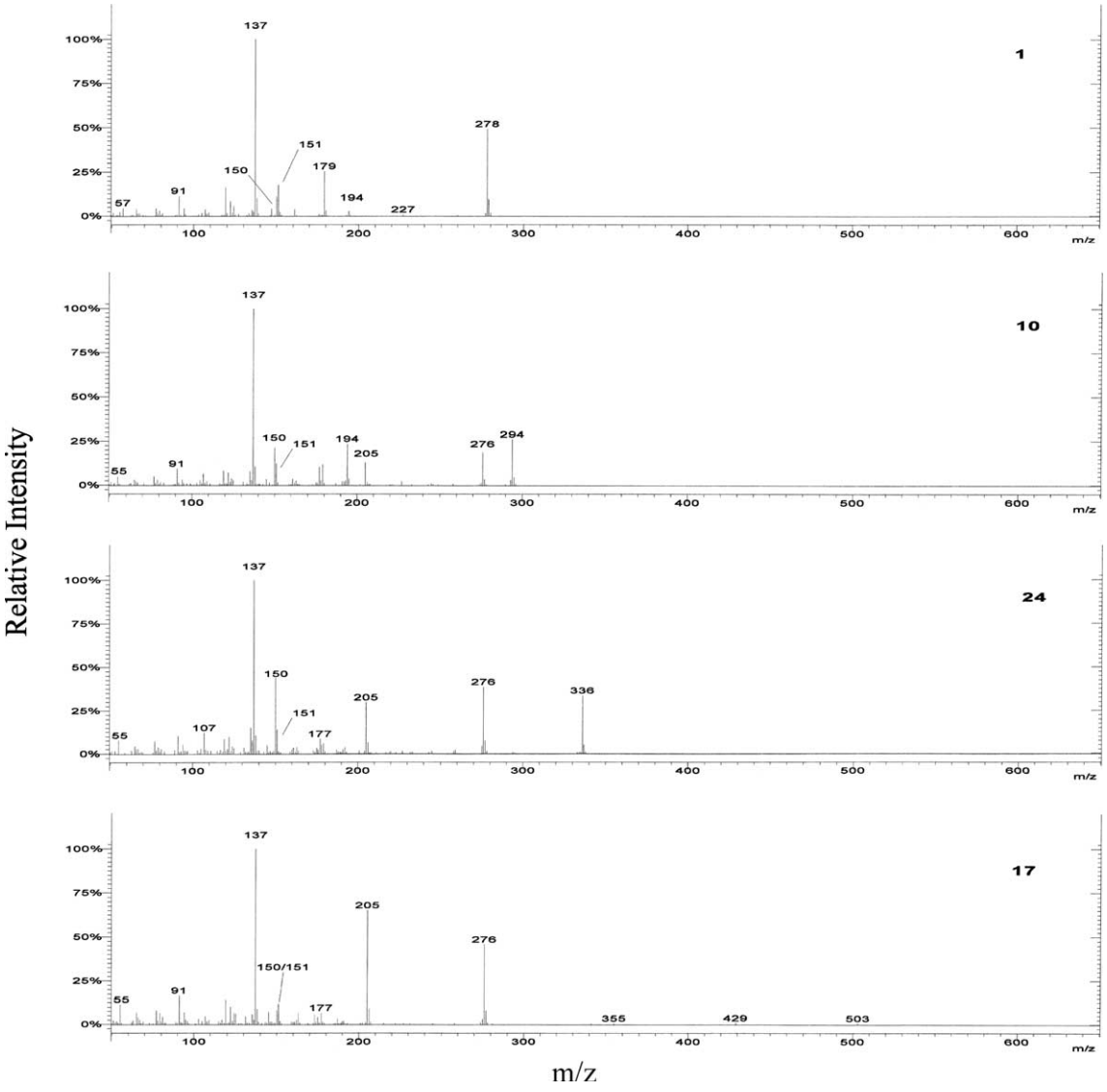

Fig. 3. Mass spectra of compounds **1**, **10**, **24** and **17** listed in Table 2.

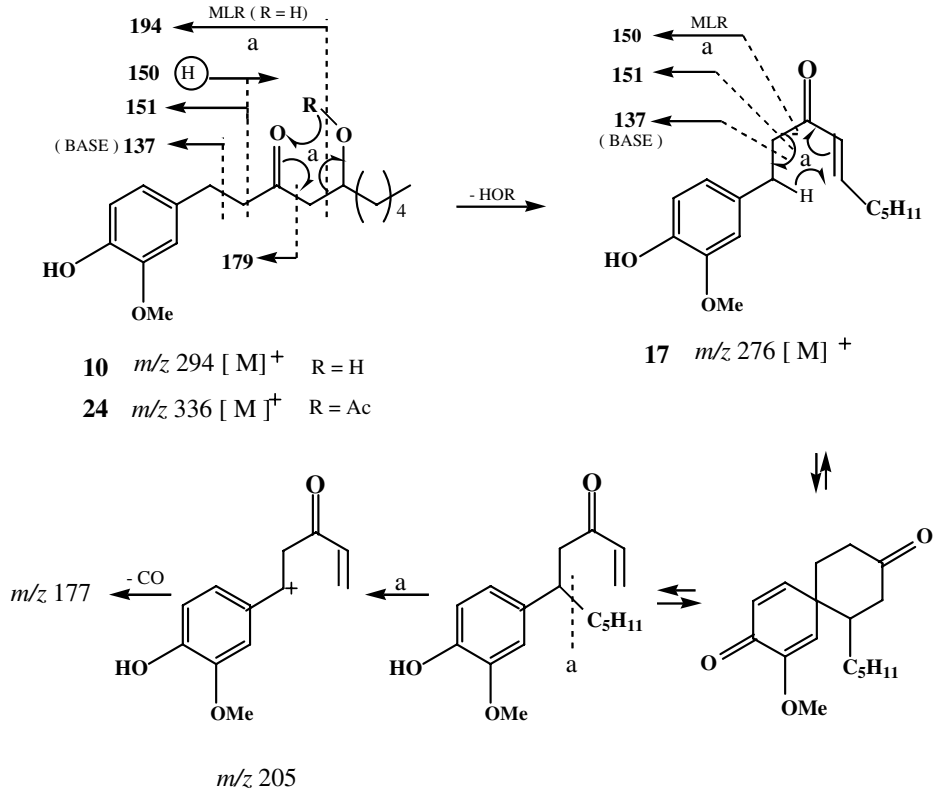

Scheme 1. Major fragment ions in the mass spectra of [6]-gingerol (**10**) Ac-[6]-gingerol (**24**) and [6]-shogaol (**17**).

detected (Fig. 2). Two additional peaks in the chromatogram are thought to be due to [6]- and [8]-shogaols (**10** and **12**) based on their $[M]^+$ and very close Rt. Their spectra were very similar to those of [6]- and [8]-shogaols (**10** and **12**) except for the presence of an MLR peak at m/z 194 (Fig. 4), suggesting that they could be the isomeric form of [6]- and [8]-shogaols (**54** and **55**) presumably formed from gingerols via dehydration followed by isomerization under the GC conditions. Another fraction (GF3-F11), which contained [10]-gingerol (**13**) as the major constituent by HPLC, showed [10]-shogaol (**20**) as the major component with no trace of [10]-gingerol (**13**) in its GC chromatogram. Similarly, fraction GF3-F13, which contained [6]-gingerol (**10**) as the major peak and a trace of [10]-gingerol (**13**) by HPLC, displayed in its GC chromatogram [6]-gingerol (**10**) as the major peak along with minor peaks corresponding to **54**, **58** and **60**. It is concluded from the above results that the higher members of gingerol homologs ($n > 8$), because of their long retention times (even at temperatures as high as 250 °C), undergo complete thermal dehydration while the lower members suffer partial dehydration and isomerization as well. Despite the thermal formation of shogaols (and isomers) from gingerols under the GC conditions they also co-occur with gingerols as natural ginger constituents as demonstrated by the HPLC/LC–MS analysis of the CC fractions.

No peak associated with zingerone (**60**) was detected in any of the nonpolar fractions but its appearance and dramatic increase in abundance was observed in the polar fractions (see Fig. 2), especially two [6]-gingerol (**10**) enriched fractions (GF2-F13 and GF2-F14) in which zingerone (**60**) appeared as the major peak. It appears, therefore, that zingerone (**60**) is not a natural ginger constituent but an artifact (could be a retro-aldol product) formed from [6]-gingerol (**10**) and/or its analogs under the GC conditions, an inference supported by the LC–MS in which no zingerone was detected. Similarly, other compounds listed in Table 3, like zingerone (**60**), appeared to be artifacts since none of them were detected by LC–MS.

The presence of methyl-[6]-gingerol (**15**) was recognized from all the diagnostic peaks of [6]-gingerol (**12**), m/z 294 $[M]^+$ (***308***), 276 (***290***), 205 (***219***), 194 (***208***), 151 (***165***), 150 (***164***) and 137 (base) (***151***, ***base***), shifted upward by 14 mass units in its GC–MS spectrum, shown in italic boldface. However, despite these peak shifts the presence of pronounced peaks at m/z 137 (91%), 194 (35%) and 205 (11%) together with the absence of a [6]-gingerol $[M]^+$ peak at m/z 294 clearly suggested that it contains [7]-gingerol (**11**) as an unresolved mixture. The occurrence of a base peak at m/z 151 (shifted from m/z 137 in **10**) clearly shows that the OH group in the aromatic ring is methylated in **15**. Methyl [4]-gingerol (**14**) was identified similarly. The presence of [4]-gingerol (**9**)

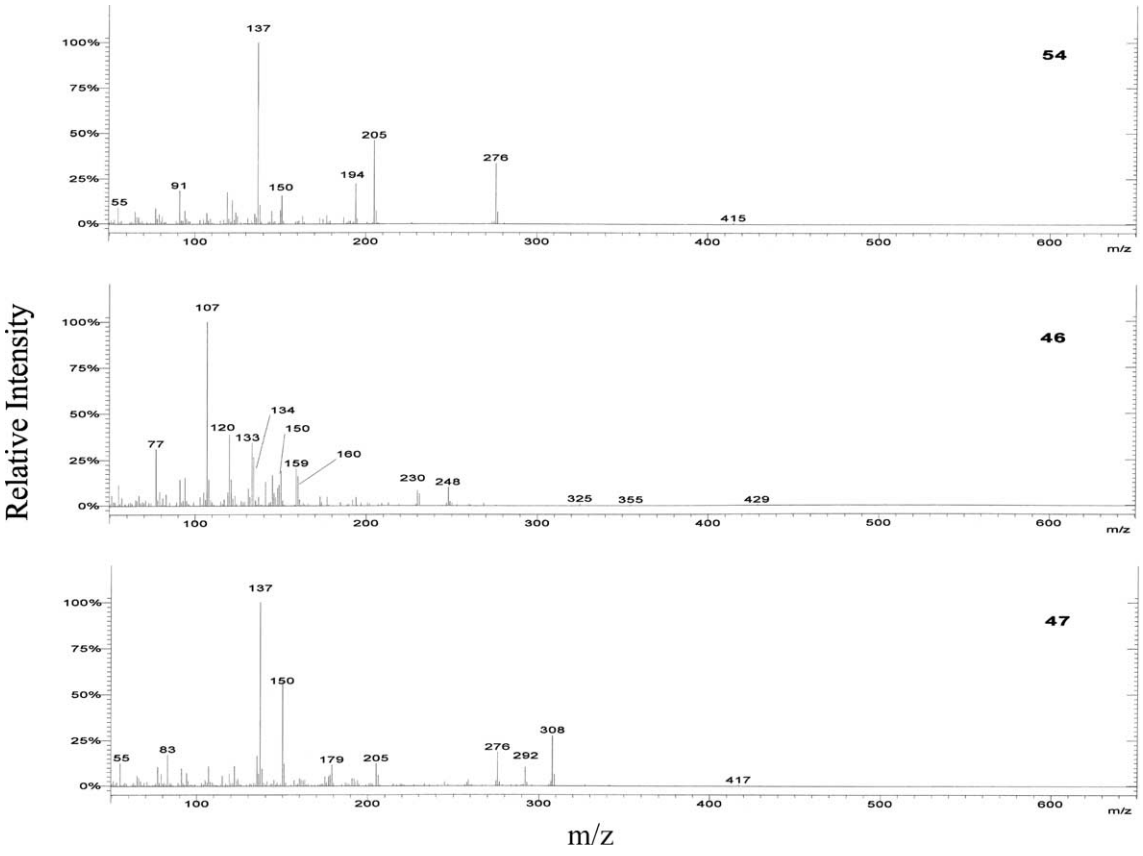

Fig. 4. Mass spectra of compounds **54**, **46** and **47** listed in Table 2.

was observed in GF2-00 and GF3-00 but its methyl ether derivative (**14**) and isomer (**56**) were detected only in GF2-00, the latter for the first time. The mass spectrum of **56** with a base peak at m/z 137 was very similar to that of **9** (Fig. 5) except for the MLR peak at m/z 194 which was shifted downward by 14 mass units to m/z 180 and the appearance of peaks at m/z 163 and 162. These key fragments led us to postulate that **56** possesses

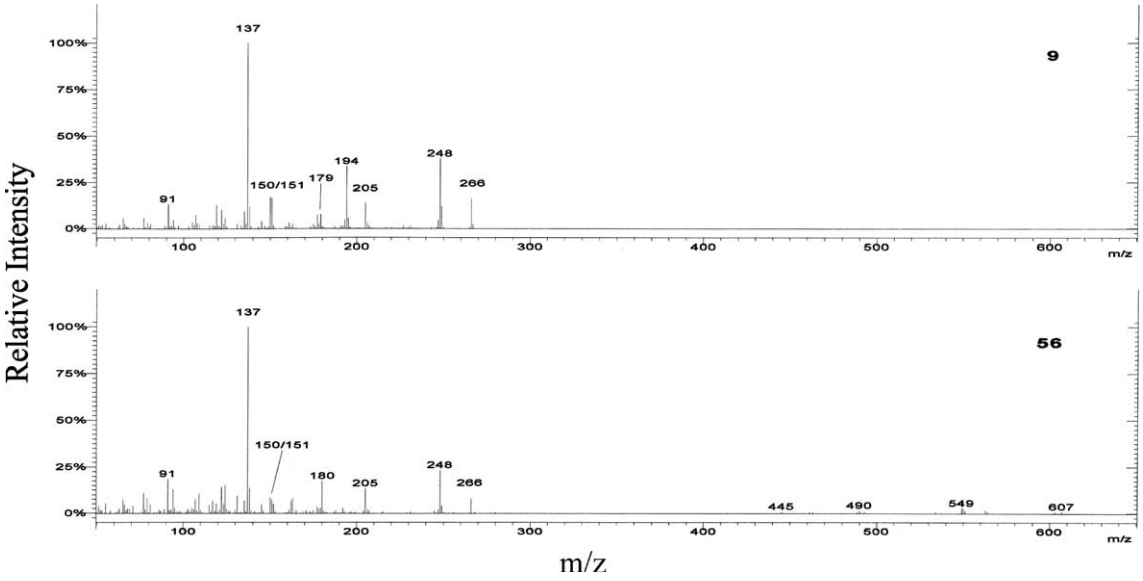

Fig. 5. Mass spectra of compounds **9** and **56** listed in Table 2.

the same skeletal framework as **9** except for the substituents at C-3 and C-5 in **9** which are switched in **56** as shown and ruled out a demethyl-[5]-gingerol structure.

2.3. Shogaols (16–22)

Shogaols (**16–22**) were readily recognized by the presence of three peaks which dominated their spectra: an intense $[M]^+$ peak, a base peak at m/z 137 and a striking peak at m/z 205 with high abundance resulting from cleavage of the C-5/C-6 bond as rationalized in Scheme 1. Additional diagnostic peaks at m/z 177 (m/z 205-CO) and 150/151 (C-2/C-3 cleavage with and without H transfer) were seen as a minor fragmentation process. The GC–MS spectrum of [6]-shogaol (**17**), reproduced in Fig. 3, serves as a typical example. The existence of homology within the family of [*n*]-shogaols ($n = 4$, 6, 8, 10 and 12) was clearly seen in their GC–MS spectra. The presence of [6]-shogaol (**17**) was also identified by HPLC using a reference standard. In the methylated derivatives of shogaols (**21–22**), all the fragment ions observed for their parent compounds shifted upward by 14 mass units.

2.4. Paradols (1–8)

Paradols are 5-deoxygingerols. The GC–MS spectrum of [6]-paradol (**1**), reproduced in Fig. 3, shows a typical paradol fragmentation pattern. An abundant $[M]^+$ peak, a base peak at m/z 137, a C-3/C-4 fission peak at m/z 179, a pair of peaks at m/z 150/151 and an MLR peak at m/z 194 were the main GC–MS features of [*n*]-paradols. Except for [12]-paradol, which was not detected, the family of [*n*]-paradols ($n = 6$ to 11 and 13) clearly demonstrated the homologous relationship in their GC–MS spectra. In the methylated derivative of [6]-paradol (**8**), the above characteristic peaks observed in the parent molecule (**1**) now occurred with increments of 14 mass units [m/z 292 $[M]^+$, 208, 193, 165/164 and 151 (base)], suggesting that the OH group in the aromatic ring is methylated. Reported for the first time are [11]- (**6**), [13]- (**7**) and methyl [6]- (**8**) paradols. Compound **8** is known only by synthesis (Galal, 1996).

2.5. Gingerol acetates (23–27)

The four acetyl gingerol homologs (**23–27**), which contain an acetyl group at C-5, behaved very much the same way as the shogaol homologs after the deacetylation step. They exhibited an intense $[M]^+$ peak at m/z 308 (in **23**), 336 (in **24**), 364 (in **25**) and 392 (in **26**), represented by their daughter ions (M-HOAc) at m/z 248 (in **23**), 276 (in **24**), 304 (in **25**), and 332 (in **26**), the molecular ion peaks of [4]-, [6]-, [8]-, and [10]-shogaols, respectively, and the rest of their spectra nearly superimposed on the GC–MS spectra of the four shogaols (**16–19**). The methylated derivative of [6]-gingerol acetate (**27**) showed all the expected ions [m/z 350 $[M]^+$, 290, 219, 191, 177, 165/164 and 151 (base)] shifted to upper mass units by 14. The GC–MS spectrum of [6]-gingerol acetate (**24**), reproduced in Fig. 3, serves as a typical example. Reported for the first time are compounds **23**, **25** and **26.**

2.6. Gingerdiols (32–35)

The presence of four gingerdiol homologs (**32–35**) was marked by their successive double dehydration process from $[M]^+$ exhibiting $[M]^+$ peak homology at m/z 268 (in **32**), 296 (in **33**), 324 (in **34**) and 352 (in **35**), a strong (M-H_2O) peak followed by a weak but discernible (M-2H_2O) peak. The presence of these two subsidiary peaks, a base peak at m/z 137, and very similar fragmentation pattern in the lower mass region of their spectra allowed their identification as [4]-, [6]-, [8]-, and [10]-gingerdiols (**32–35**). Further support came from the reported EIMS m/z values for [6]-gingerdiol [isolated from *Z. officinale* (Kikuzaki et al., 1992)] which are in accord with the GC–MS spectral values [m/z 296 $[M]^+$, 278 (M-H_2O), 260 (M-2H_2O), 207, 190/189, 180, 175, 164/163, 151/150, and 137(base)]. The GC–MS spectrum of [6]-gingerdiol (**33**), reproduced in Fig. 6, serves as a typical example.

2.7. Monoacetyl derivatives of gingerdiols (36–40)

Monoacetyl derivatives of gingerdiols (**36–40**) exhibited identical diagnostic peaks for all the structural elements of gingerdiols following the deacetylation and dehydration steps. The presence of two auxiliary peaks, (M-HOAc) and (M-HOAc-H_2O), clearly indicated that one of the two OH groups in gingerdiols is replaced by an acetate group. This suggests that the fragmentation routes in gingerdiols and monoacetyl derivatives of gingerdiols eventually leads to common ions after initial dehydration and deacetylation, respectively. The GC–MS spectrum of 5-acetoxy-[6]-gingerdiol (**37**), reproduced in Fig. 6, serves as a typical example. The isolation and identification of **37** from *Z. officinale* has been reported (Kikuzaki et al., 1992) but as an unresolved mixture with its isomer (OAc at C-3). The EIMS m/z values of this mixture are in accord with our GC–MS data. The presence of methylated derivatives of gingerdiol monoacetates (**39–40**) was recognized from the characteristic peaks that occur upward by 14 mass units. This paper constitutes the first report of detection of compounds **36** and **38–40.**

2.8. Diacetyl derivatives of gingerdiols (41–45)

The diacetates of gingerdiols (**41–42**) and the methylated derivatives (**43–45**) fragmented in an identical fashion exhibiting peaks basically similar to those

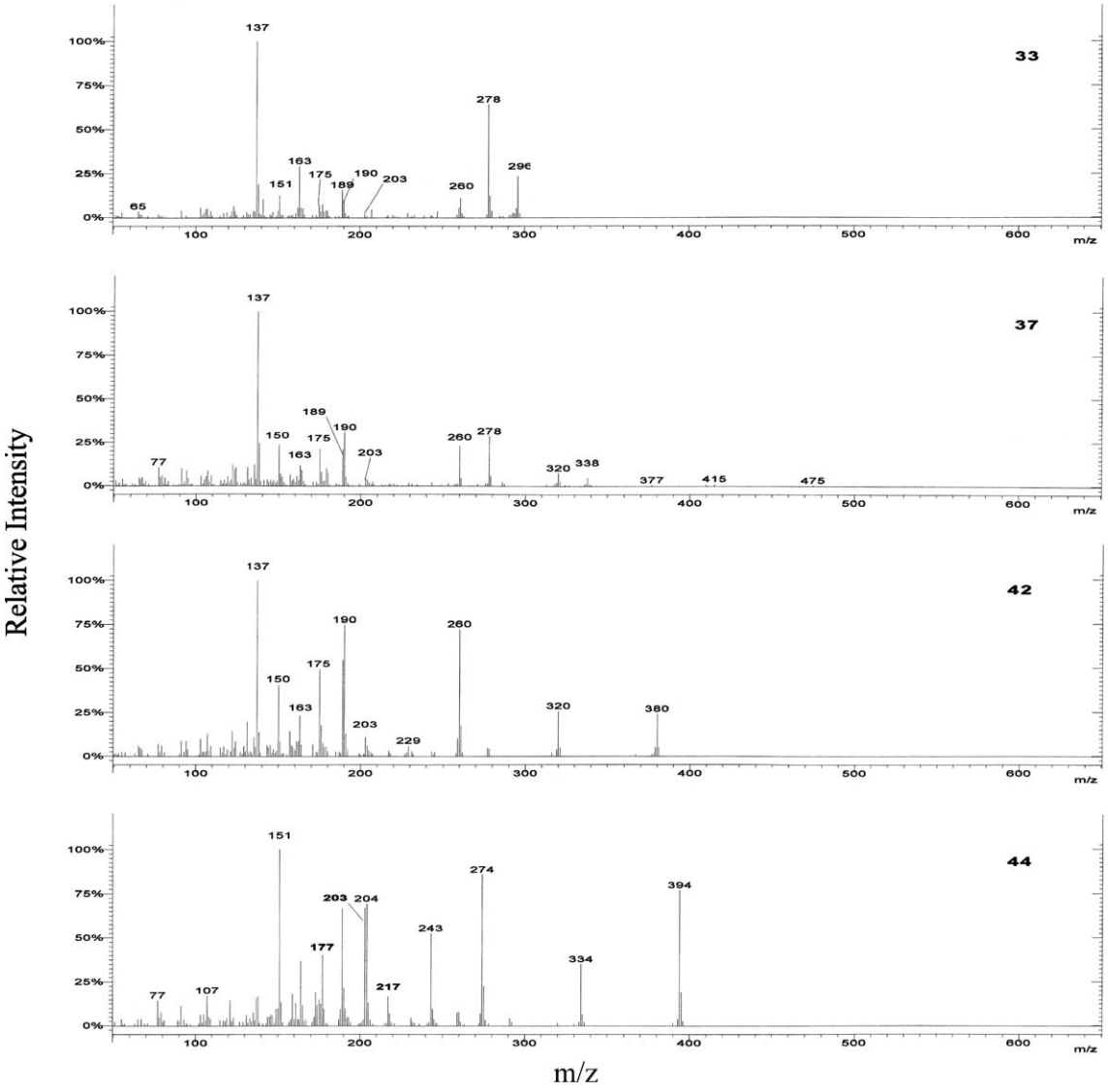

Fig. 6. Mass spectra of compounds **33**, **37**, **42** and **44** listed in Table 2.

which appeared in the spectra of gingerdiols following the elimination of two elements of acetic acid from $[M]^+$ except that the peaks in **43**–**45** were more pronounced than those in **41**–**42** and shifted upward by 14 mass units. The GC–MS spectra of [6]-gingerdiol diacetate (**42**) and its methylated derivative (**44**) are reproduced in Fig. 6. Compounds **41** and **42** are known to occur in Japanese and Chinese gingers as demonstrated not only by the GC–MS analysis of a fraction modified to the TMS derivative (Masada et al., 1974) but also by their isolation and identification by spectral analysis (Kikuzaki et al., 1992). The reported EIMS m/z values for **41** and **42** are in accord with our data (Scheme 2).

2.9. Dehydrogingerdiones (*28*–*31*)

The isolation and spectral identification of 1-dehydro-[6]-gingerdione (**29**), m.p. 84–85 °C, from *Z. officinale* has been recently reported (Charles et al., 2000). Our compound had the same mp and its ^{1}H NMR spectral data were in accord with the reported data. The GC–MS data of our sample, however, was not in full accord with the reported EIMS data. The reported fragment ions for **29** at m/z 290 $[M]^+$, 219, 191 and 177 (base) were observed in the GC–MS spectrum of our sample but the most striking difference compared with the EIMS of **29** was the occurrence of a strong peak at m/z 272 followed by pronounced peaks at m/z 216, 201, 145 and 117 as shown in Fig. 7. The formations of these peaks are rationalized in Scheme 3. This very characteristic behavior of **29** under GC–MS conditions offered a simple means to detect and identify the presence of its homologs (**30**–**31**) which exhibited nearly superimposable spectra with $[M]^+$ and $(M\text{-}H_2O)$ peaks shifted upward by 28 mass units (318/300 in **30** and 346/328 in **31**). Interestingly, similar high intensity peaks at m/z 177,

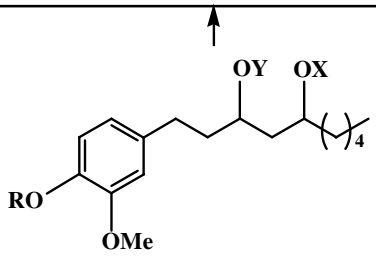

	33	37	42	44
[M]$^+$	296	338	380	394
R	H	H	H	Me
X	H	Ac	Ac	Ac
Y	H	H	Ac	Ac
		- HOX		
m/z	278	278	320	334
		- HOY		
m/z	260	260	260	274
m/z	203	203	203	217
m/z	190	190	190	204
m/z	189	189	189	203
m/z	175	175	175	189
m/z	163	163	163	177
m/z (base)	137	137	137	151
m/z	151	150	150	150

Scheme 2. Diagnostic fragment ions in the mass spectra of [6]-gingerdiol (**33**), Ac-[6]-gigerdiol (**37**), DiAc-[6]-gingerdiol (**42**) and MediAc-[6]-gingerdiol (**44**).

145 and 117 were reported in the EIMS of 1-dehydroshogaol homologs ([6], [8] and [10]) isolated and characterized from *Z. officinale* (Wu et al., 1998). The presence of abundant peaks at m/z 192 (via MLR), 177, 161/160 (192-MeOH), 145 (base) and 117 together with an intense $[M]^+$ peak at m/z 248 followed by a subsidiary peak at m/z 219 in the GC–MS spectrum of **28** immediately suggested that this compound is 1-dehydro-[3]-gingerdione. Surprisingly, the dehydration peak, which is the precursor for the formation of ions at m/z 216 and 201 in **30–31** as shown in Scheme 3, was not seen in **28**. The absence of a M-H_2O peak and the lack of a γ-hydrogen available for MLR explains the absence of peaks at m/z 216 and 201 in **28**. The GC–MS spectrum of **28**, a synthetic product (Belliotti et al., 1987) but reported here from a natural source for the first time, is reproduced in Fig. 7. Compounds **30** and **31** have been previously isolated from *Z. officinale* and characterized by ^{1}H and ^{13}C NMR (Masanori et al., 2002).

2.10. Diarylheptanoids (*48–49*)

Two diarylheptanoids (**48** and **49**), were detected in the high Rt region of the GC–MS. The shogaol equivalent of diarylheptanone, gingerinone A (**48**), showed an $[M]^+$ peak at m/z 356 with appreciable intensity. Besides the base peak at m/z 137, three pairs of peaks (m/z 151/205, 150/206, and 137/219) adding up to the *Mr*, two daughter ions of m/z 206 at m/z 162/163 and a discernible but diagnostic peak at m/z 179 supported our identification. The isolation, spectral and chemical characterization of **48** from *Z. officinale* has been reported (Endo et al., 1990). Mass spectral fragmentation data for this compound is not reported but for a compound in which the 4′-hydroxy-3′-methoxyphenyl group at C-7 in **48** is replaced by a 3′,4′-dihydroxyphenyl moiety, similar fragment ions are reported in addition to the ion representing this moiety (Kikuzaki et al., 1991).

The gingerdione equivalent of diarylheptanoid **49**, like **48**, exhibited a strong $[M]^+$ peak at m/z 372, 16 mass units higher than **48**, a base peak at m/z 137, two pairs of peaks (m/z 179/193 and 151/221) adding up to the *Mr*, but the peaks at m/z 162/163 and 205/206 observed in **48**, were completely suppressed suggesting the absence of a double bond between C-4/C-5 in **49**. Instead, a weak peak occurred at m/z 194, the product of MLR, not observed in **48**. These data supported the designated structure for **49**, a tetrahydrocurcumin derivative prepared from curcumin (Somepalli et al., 2000) but not hitherto reported as a constituent of ginger.

2.11. Miscellaneous compounds

2.11.1. Compound *50*

This compound exhibited a $[M]^+$ peak at m/z 348, suggesting that it could be a reduction product of co-occurring 1-dehydro-[10]-gingerdione (**31**) in which either the double bond between C-1 and C-2 is reduced to form [10]-gingerdione [reported from *Z. officinale* (He et al., 1998)] or one of the two keto groups was reduced to form a secondary alcohol. The former was ruled out based on the presence of two key fragment ions, the dehydration peak at m/z 330 and 4′-hydroxy-3′-methoxycinnamoyl cation as the base peak at m/z 177 represented by two daughter ions at m/z 145 and 117 – a feature of the GC–MS of all 1-dehydrogingerdiones

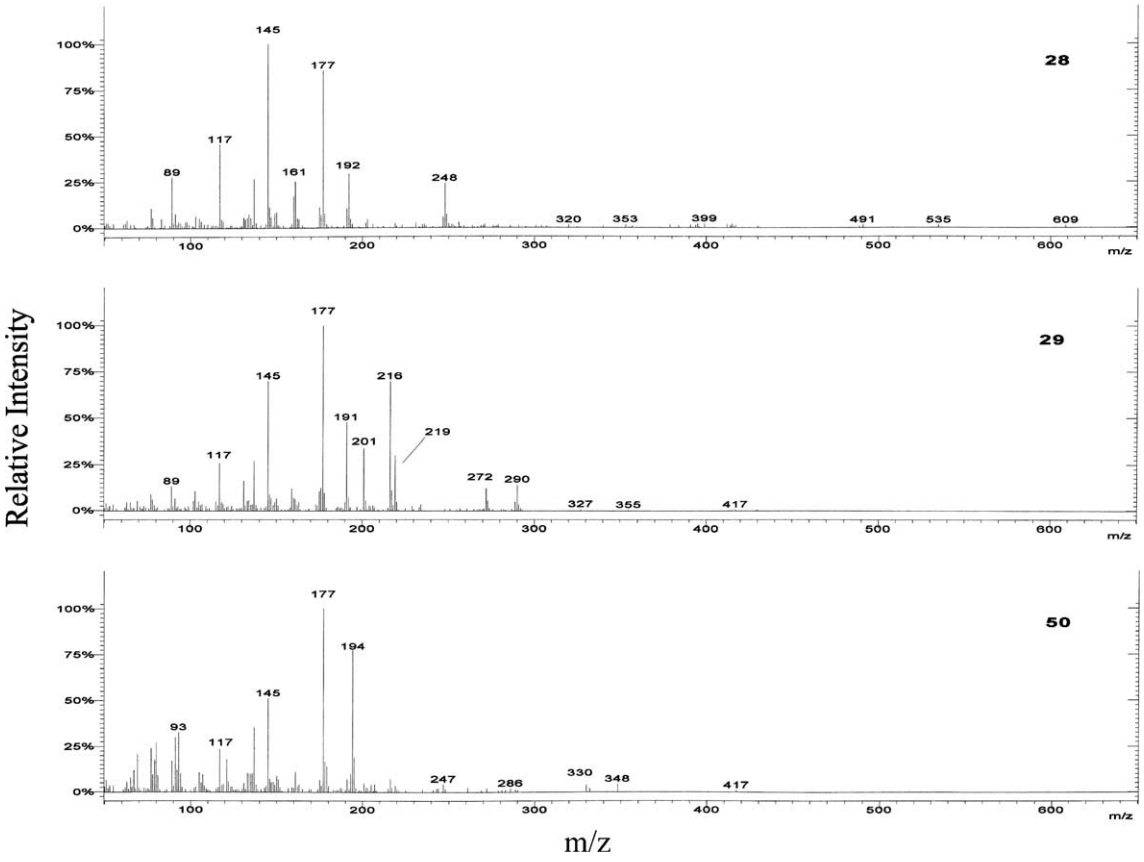

Fig. 7. Mass spectra of compounds **28**, **29** and **50** listed in Table 2.

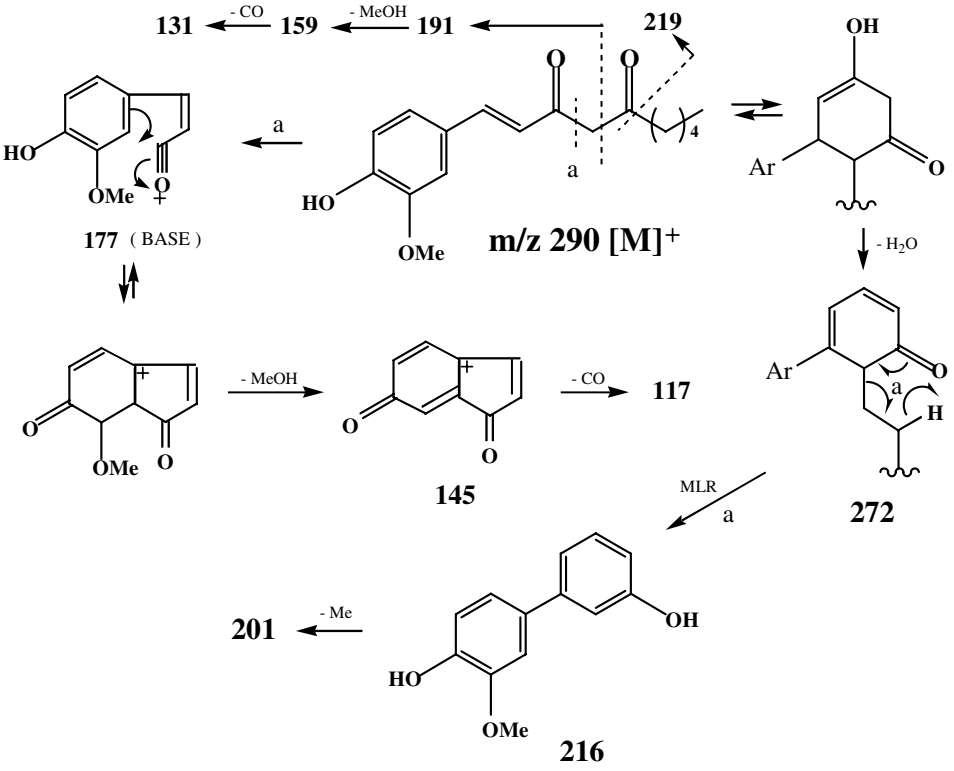

Scheme 3. Major fragment ions in the mass spectrum of 1-dehydro-[6]-gigerdione (**29**).

detected in this investigation. Though the site for the OH group at C-5 is more favorable since 1-dehydro-[10]-shogaol, a naturally occurring compound isolated from *Z. officinale*, could arise from **50** *via* dehydration and because of the ease of formation of the base peak at m/z 177, but no MLR peak at m/z 192, a notable feature of the GC–MS of [*n*]-gingerols, was seen and the mass spectral data reported for 1-dehydro-[10]-shogaol (Wu et al., 1998) were not fully compatible, especially the occurrence of an abundant ion at m/z 194 (82%) in **50**. The structure with the OH group at C-3 permits the generation of the two key fragments (m/z 177 and 194) as rationalized in Scheme 4. Compound **50** (its GC–MS is reproduced in Fig. 7) is therefore, identified as 1-dehydro-3-dihydro-[10]-gingerdione. Its verification by synthesis would be desirable.

2.11.2. Compounds *51* and *52*

Compound **51** (Fig. 8) gave an intense $[M]^+$ peak at m/z 280 followed by an equally pronounced dehydration (M-H_2O) peak at m/z 262, suggesting **51** is either a gingerol homolog, [5]-gingerol, or a reduction product of [6]-paradol in which the keto group at C-3 is reduced to a secondary alcohol. The possibility of **51** being [5]-gingerol was readily ruled out based on its fragmentation pattern, especially the occurrence of an abundant peak at m/z 131, a base peak at m/z 138 (represented by a daughter ion at m/z 123) in addition to the usual peak at m/z 137 (99%), two pronounced peaks at m/z 163 and 150 (represented by a daughter ion at m/z 122), and the absence of MLR peak at m/z 194 – a feature of the GC–MS of all the [*n*]-gingerols detected in this investigation. These features were reminiscent of the fragmentation pattern of gingerol (**62**), a thermal degradation product of gingerols. The genesis of m/z 131 from m/z 163 via the elimination of MeOH, similar to the formation of m/z 145 from m/z 177 via the loss of MeOH proposed in Scheme 3, is invoked to locate the OH group in **51**. This rationale was supported by another compound (**52**) which displayed a strong $[M]^+$ peak at m/z 322, 42 mass units more than **51**, an abundant auxiliary (M-HOAc) peak at m/z 262 (95%) and a spectrum showing all the characteristic mass spectral features of **51** except for changes in the relative intensities of the peaks (see Fig. 8). This indicated **52** to be a monoacetate of **51**.The location of the OH group at C-3 in **51** comes from a peak at m/z 177, barely seen in **51** but with appreciable intensity in **52**, resulting from cleavage of the C-4/C-5 bond after dehydration/deacetylation. Compound **51** was reported previously (Masada et al., 1974) as a synthetic as well as an enzymatic reduction product of [6]-shogaol (Surh and Lee, 1992).

2.11.3. Compound *46*

This compound exhibited a $[M]^+$ peak at m/z 248, same as the $[M]^+$ peak of [4]-shogaol (**16**) and 1-dehydro-[3]-gingerdione (**28**) but both were immediately discounted from the breakdown pattern. Its base peak at m/z 107, 30 mass units lower than the base peak at m/z 137 observed in all the compounds referred to above, clearly suggested that **46** contains the demethoxyphenyl moiety $HOC_6H_5CH_2$. Confirmation came from the revelation that, in addition to the dehydration peak at m/z 230, all the major characteristic fragment ions seen in 5-acetoxy-[6]-gingerdiol (**37**, m/z 338 $[M]^+$, shown in parenthesis and in boldface) were also present in **46** but shifted downward by 30 mass units (m/z 248 $[M]^+$) (**278**, **M-HOAc**), 230 (M-H_2O), [260 (**278-H_2O**)], 160 (**190**), 159 (**189**), 150 (**180**), 149 (**179**), 134 (**164**), 133 (**163**), 120 (**150**) and 107 (base) (**137**, **base**). This fragmentation behavior of **46** (Fig. 4), analogous to the behavior of **37**, together with the detection of **57**, a thermal degradation product, sufficed to permit recognition of **46** having the structure shown in Table 2. Reported for the first time as a natural product is **46**.

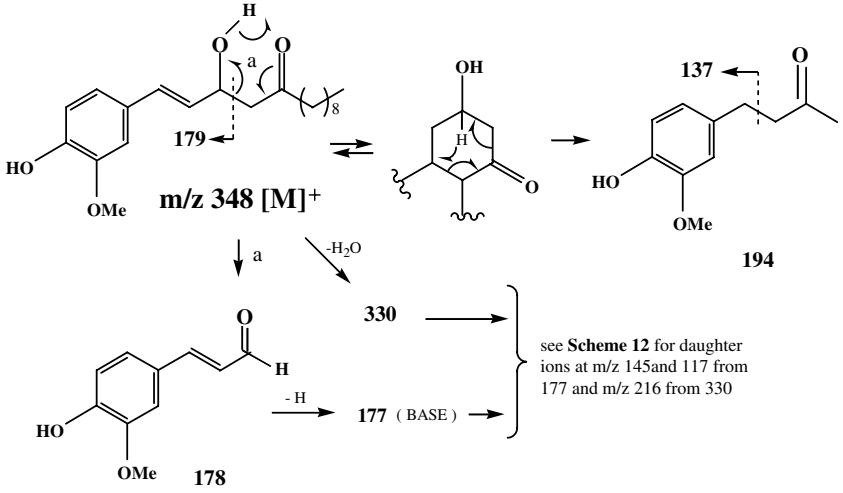

Scheme 4. Major fragment ions in the mass spectrum of 1-dehydro-3-dihydro-[10]-gigerdione (**50**).

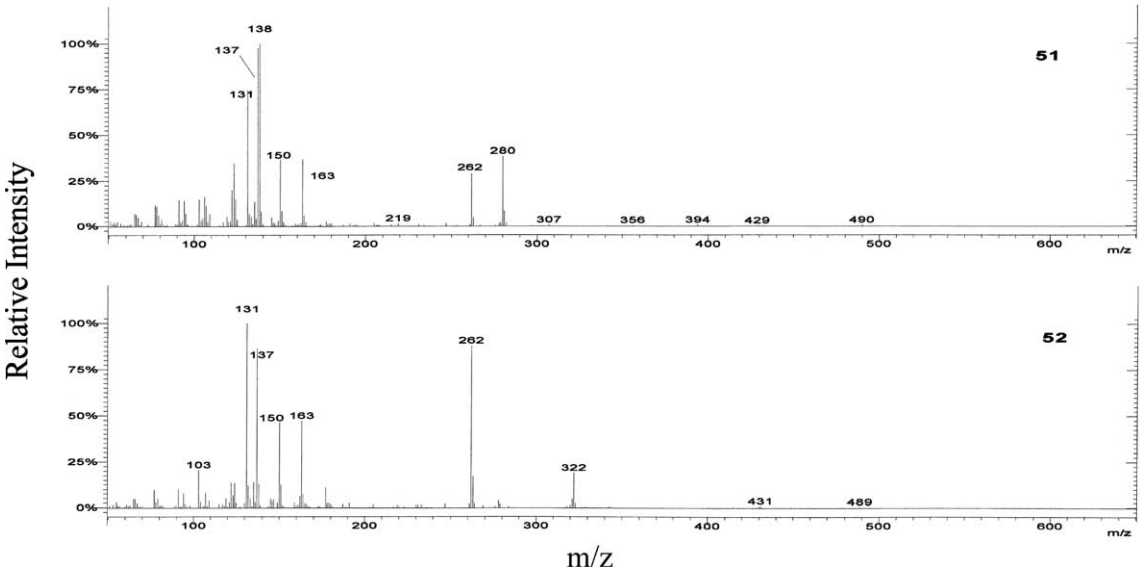

Fig. 8. Mass spectra of compounds **51** and **52** listed in Table 2.

2.11.4. Compounds 53–55

The occurrence of $[M]^+$ peaks at m/z 248 in **53**, 276 in **54** and 304 in **55**, same as the $[M]^+$ peak of [4]- (**16**), [6]- (**17**) and [8]- (**18**) shogaols, respectively, together with distinctive peaks at m/z 205 and 137 (base) were reminiscent of the fragmentation behavior of [*n*]-shogaols, offering strong evidence for **53**–**55** possessing the [4]-, [6]- and [8]-shogaol carbon skeletons, respectively. But the position of the double bond between C-3 and C-4 as in shogaols was ruled out based on the presence of an MLR peak at m/z 194, which stands out in all three spectra, a feature of the GC–MS of [*n*]-gingerols in which the OH group at C-5 is a requisite for MLR. However, **53**–**55**, which displayed superimposable spectra below the $[M]^+$ peak with no dehydration peak, clearly suggested that they contained no OH group. These mass spectral evidences pointed strongly towards a shogaol skeleton with the double bond placed as shown in Scheme 5, the only structure that permits the generation of both key fragments at m/z 205 and 194. The fact that **53**–**55** are not [4]-, [6]- and [8]-shogaols, respectively, came because the HPLC chromatogram of the fractions in which these compounds were detected by GC–MS (**54** and **55** in GF3-F12 and **53** in GF3-F14) exhibited none of the peaks that corresponded to [4]-, [6]- and [8]-shogaols although their retention times in the GC chromatogram plots were very close [21.075 (**53**)/21.080 (**16**), 22.927 (**54**)/22.965 (**17**), 24.682 (**55**)/24.678 (**18**)]. Hence the possibility that **53**–**55** might be the isomeric forms of shogaols formed from gingerols under the conditions of gas chromatography was not ruled out; substantiation requires synthesis and further study. The GC–MS spectrum of **54**, reproduced in Fig. 4, is shown as a typical example.

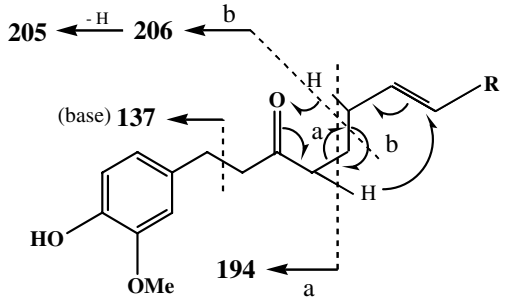

	$[M]^+$	R
53	248	H
54	276	CH_2Me
55	304	$(CH_2)_3Me$

Scheme 5. Major fragment ions in the mass spectrum of **53**–**55**.

2.11.5. Compound 47

The occurrence of an $[M]^+$ peak in the MS of the new compound **47** (Fig. 4) at m/z 308 (14 mass units more than **10**), the loss from $[M]^+$ of 32 mass units, equivalent to MeOH (m/z 276, the $[M]^+$ peak of **17**), and the presence of peaks at m/z 205 (diagnostic peak in [*n*]-shogaols), 151/150 and 137 (base) sufficed to permit recognition of the side chain OH at C-5 in **10** being methylated, a deduction strongly supported by the absence of a MLR peak at m/z 194. A peak at m/z 292, appears to come from the loss of CH_4.

Except for major differences in the amounts of [6]-, [8]- and [10]-gingerols (**10**, **12** and **13**), notably [6]-gingerol (**10**), and minor variations in the amounts of a few minor constituents, the white and yellow ginger

varieties appeared to be basically similar, as can be seen from the two chromatograms reproduced in Fig. 9. Judging from the very low concentration of [*n*]-shogaol compared to the high concentration of gingerols in the two fresh ginger varieties, shogaols seem to originate in nature as minor constituents. [*n*]-Gingerols, without modification, undergo degradation to zingerone and related products as well as dehydration to the corresponding [*n*]-shogaols. Lower homologs ($n \leqslant 8$) suffer partial dehydration followed by partial isomerization of the dehydrated products, while higher homologs ($n \geqslant 10$) completely convert to the corresponding shogaols. Whether the [*n*]-paradols (**1**–**8**) are derived in nature from the reductive degradation of [*n*]-shogaol precursors or produced artificially during the commercial production of ginger requires further study.

3. PGE_2 production and cytotoxicity

Of the CC fractions analyzed for biological activity, cytotoxicity only occurred at fairly high doses (greater than 50 μg/ml; Table 1). Therefore, inhibition of PGE_2 production was not due to the toxicity of the fractions. All of the fractions analyzed had high activity (IC_{50} between 50 and 100 ng/ml). This is comparable to the IC_{50} for indomethacin in our assay system. Tjendraputra et al. (2001) have demonstrated that pure compounds found in ginger have varying abilities to inhibit PGE_2 production. The inhibition depended on the length of the carbon chain as well as the presence of modifying groups. Our studies show lower IC_{50} values than those reported by Tjendraputra et al. (2001) by more than an order of magnitude. This could be due to use of different cell types in the in vitro assay or to the fact that our tests were performed on mixtures of ginger constituents rather than on pure compounds.

4. Experimental

4.1. Plant material

Chinese white and Japanese yellow ginger seed rhizomes were planted in March 2002 and the resulting plants were grown amended only with organic fertilizer at Hilo Hawaii for the next several months. Mature rhizomes from these plants were harvested in March 2003, two days prior to shipment to Tucson, Arizona, for storage (two weeks at 4 °C) and subsequent chemical analysis.

4.2. Extraction

Rhizomes of the yellow variety (GF3, 3.3 kg) were sliced into small pieces, blended with MeOH (10 l) and stirred mechanically for 18 h at RT. The liquified ginger was filtered and after washing the marc with fresh MeOH, the organic phase from the combined filtrate and washings was stripped off. The remaining aq. phase was diluted with water and the oily content was extracted with CH_2Cl_2 to afford 17.9 g (0.54%; GF3_00). Further extraction of the aq. phase with *n*-butanol provided an additional 1.72 g (0.052%; GF3_ZZ). Repetition of the above procedure under identical conditions with rhizomes of the white variety (GF2, 3372 g) afforded 16.56 g (0.49%) of CH_2Cl_2 extract (GF2_00) and 2.22 g (0.062%) of *n*-butanol extract (GF2_ZZ).

4.3. Fractionation

The CH_2Cl_2 extracts of white (GF2-00;16.35 g) and yellow (GF3-00;17.5 g) gingers were fractionated by CC on silica gel following methodology developed in our laboratory for the separation of gingerols in gram quantities for in vivo assay from a commercial dry ginger powder. Multiple CC fractions collected were reduced to 20 fractions (GF2-01 through GF2-20) in the case of GF2-00 and 18 fractions (GF3-01 through GF3-18) in the case of GF3-00 based on the TLC and HPLC profiles and tested along with the originals (GF2-00 and GF3-00) and n-butanol extracts (GF2-ZZ and GF3-ZZ) for anti-inflammatory activity in the PGE_2 in vitro test system by standard ELISA assays (Lantz et al., 1995).

4.4. Gas chromatography–mass spectrometry

GC–MS data were recorded with a Varian Saturn 2100T. The gas chromatograph was fitted with a Chrompack capillary column (CP Sil 8 CB; 30 m × 0.25 mm). Operating conditions: column oven temperature programmed at 80 °C for 5 min and then to 280 °C at 10 °C/min; injector/transfer line/trap temperatures 250/250/200, respectively; electron voltage, 50–80 eV. UHP helium was used as the carrier gas at a flow rate of 1.2 ml/min. Each fraction (~1 mg) was dissolved in CH_2Cl_2 (0.5 ml) and injected (1 μl) directly into the chromatograph.

4.5. High-pressure liquid chromatography

Sample preparation: Each sample (~1–3 mg) was dissolved in a mixture of MeOH (1 ml) and CH_2Cl_2 (3 drops) and filtered through 0.45 m Nylon filter (Whatman) before injecting onto the HPLC column. Agilent 1100 HPLC system; Detector: DAD; Column: Luna C18(2), 5 μm, 250 × 4.6 mm (Phenomenex); Guard column: Security Guard AJO-4287 (Phenomenex); Mobil phase: nanopure water (A) and HPLC grade acetonitrile (B); Flow rate: 1 ml/min; Injection volume: 20 μl/inj; Detection: 210, 230 and 280 nm.

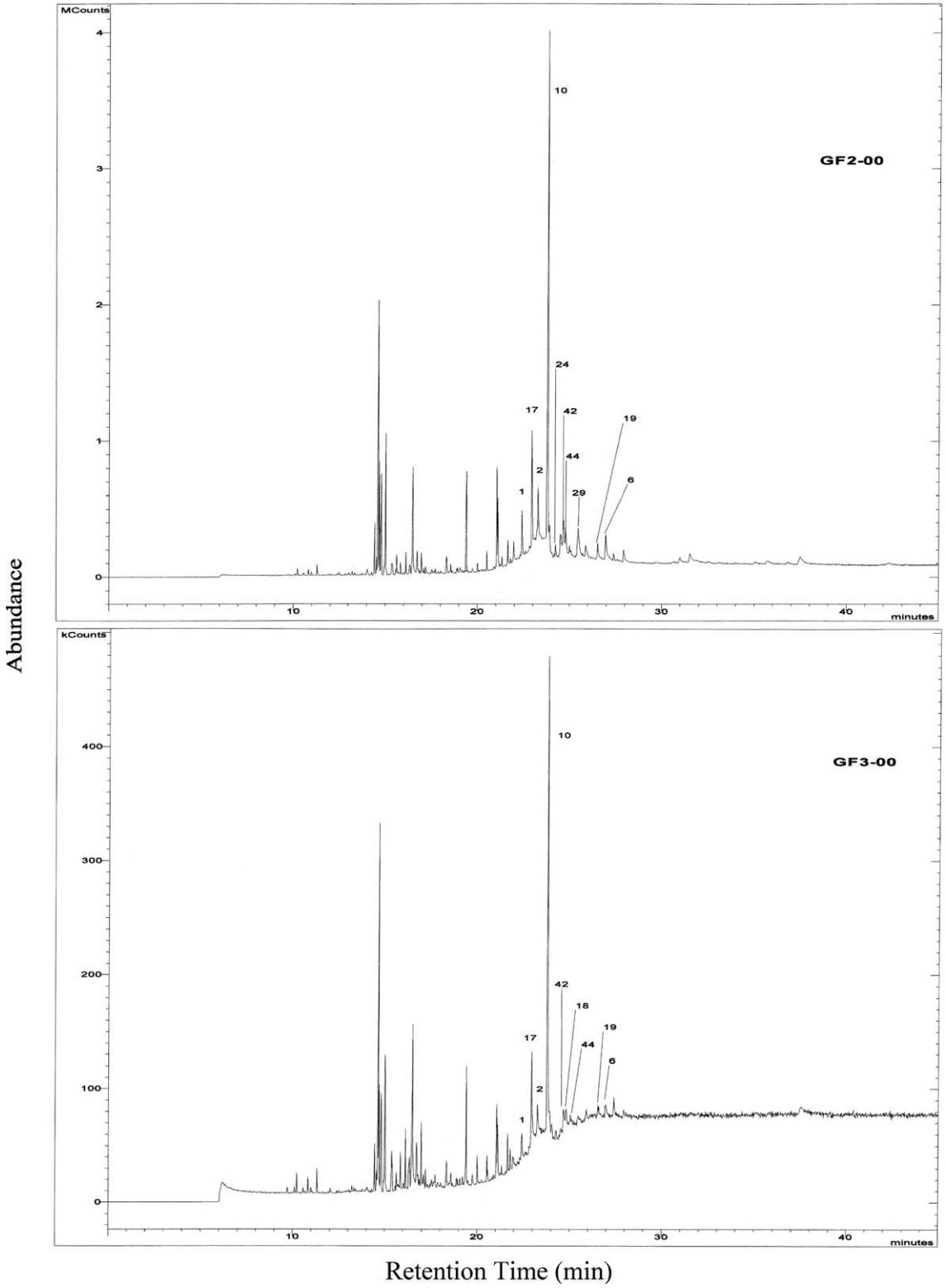

Fig. 9. GC chromatogram of dichloromethane extracts of fresh white (GF2-00) and yellow (GF3-00) ginger.

4.6. Liquid chromatography–mass spectrometry

Sample preparation: Each sample (~2 mg) was dissolved in MeOH and filtered as above. MS system: Agilent 1100 HPLC system tandem with Agilent LC-MSD-Trap-SL ion trap mass spectrometer; Column: Synergy Hydro, 4 μ, 250 × 4.6 mm (Phenomenex); Guard column: Security Guard AJO-4287

(Phenomenex); Mobil phase: 500 μl acetic acid/l of nanopure water (A) and 500 μl acetic acid/l of acetonitrile (B); Flow rate: 1 ml/min; Injection vol.: 20 μl. The acquisition parameters for MS were: positive ESI mode, drying gas temperature 350 °C, drying gas flow rate 10 l/min, nebulizer pressure 35 psi, HV capillary 3500 V, HV end plate offset −500 V, capillary current 24.4 nA, current end plate 1138.6 nA, RF amplitude capillary exit 158.5 V, skimmer 40.0 V.

4.7. Immunoassay for inhibition of PGE_2 production

The in vitro biological activity of the extracts was evaluated based on the ability of the compounds to inhibit LPS-induced production of PGE_2. HL-60 cells were stimulated with 1 μg/ml of LPS in the absence or presence of various concentrations of extracts. The concentration of extract that inhibited PGE_2 levels to 50% of the LPS alone level was used as a measure of the potency of the extracts (IC_{50}; Lantz et al., in press). None of the compounds were cytotoxic at the levels tested.

Acknowledgements

This work was supported by the National Institutes of Health ODS/NCCAM (Grant #5 P50 AT000 474-04 to B.N.T.). We wish to thank Dr. David Gang of the University of Arizona, Department of Plant Sciences, Hugh Johnson of Puna Organics and Dean Pinner of Pinner Creek Organics for generous gifts of organic white and organic yellow ginger rhizomes. We are grateful to Veronica Rodriguez for HPLC analyses and Mark Yanagihashi for preparing tables and other technical assistance.

References

Belliotti, T.R., Connor, D.T., Flynn, D.L., Kostlan, C.R., Nies, D.E., 1987. Preparation of novel styrylpyrazoles, styrylisoxazoles, and analogs as 5-lipoxygenase inhibitors. Eur. Pat. Appl., 58.

Charles, R., Garg, S.N., Kumar, S., 2000. New gingerdione from the rhizomes of *Zingiber officinale*. Fitoterapia 71 (6), 716–718.

Clark, J., Dewan, R., Locksley, H.D., Maynard, R., 1977. Pungent compounds. II. Detection and identification of paradols (alkyl 4-hydroxy-3-methoxyphenethyl ketones) by combined gas chromatography–mass spectrometry. J. Chromatogr. 134, 315–321.

Connell, D.W., McLachian, R., 1972. Natural pungent compounds. IV. Examination of the gingerols, shogaols, paradols, and related compounds by thin-layer and gas chromatography. J. Chromatogr. 67 (1), 29–35.

Connell, D.W., Sutherland, M.D., 1969. A re-examination of gingerol, shogaol, and zingerone, the pungent principles of ginger (*Zingiber officinale* Roscoe). Aust. J. Chem. 22, 1033–1043.

Endo, K., Kanno, E., Oshima, Y., 1990. Structures of antifungal, diarylheptenones, gingerenones A, B, C and isogingerinone B, isolated from the rhizomes of *Zingiber officinale*. Phytochemistry 29 (3), 797–799.

Galal, A.M., 1996. Antimicrobial activity of 6-paradol and related compounds. Int. J. Pharmacognosy 34 (1), 64–69.

Govindarajan, V.S., 1982. Ginger-chemistry, technology and quality evaluation: Part I. CRC Crit. Rev. Food Sci. Nutr. 17, 1–96.

Harvey, D.J., 1981. Gas chromatographic and mass spectrometric studies of ginger constituents: Identification of gingerdiones and new hexahydrocurcumin analogues. J. Chromatogr. 212, 75–84.

He, X., Bernart, M.W., Lian, L., Lin, L., 1998. High-performance liquid chromatography-electrospray mass spectrometric analysis of pungent constituents of ginger. J. Chromatogr. 796, 327–334.

Kikuzaki, H., Kobayashi, M., Nakatani, N., 1991. Diarylheptanoids from rhizomes of *Zingiber officinale*. Phytochemistry 30 (11), 3647–3651.

Kikuzaki, H., Tsai, S., Nakatani, N., 1992. Gingerdiol related compounds from the rhizomes of *Zingiber officinale*. Phytochemistry 31 (5), 1783–1786.

Kiuchi, F., Iwakami, S., Shibuya, M., Hanaoka, F., Sankawa, U., 1992. Inhibition of prostaglandin and leukotriene biosynthesis by gingerols and diarylheptanoids. Chem. Pharm. Bull. 40, 387–391.

Lantz, C.R., Chen, G.J., Solyom, A.M., Jolad, S.D., Timmermann, B.N., in press. The effect of turmeric extracts on inflammatory mediator production. Phytomedicine.

Lantz, C.R., Parliman, G., Chen, G.J., Barber, D., Winski, S., Carter, D.E., 1995. Effect of arsenic exposure on alveolar macrophase function. II. Effect of slightly soluble forms of As(III) and As(V). Environ. Res. 68, 59–67.

Masada, Y., Inoue, T., Hashimoto, K., Fuzioka, M., Shiraki, K., 1973. Studies on the pungent principles of ginger (*Zingiber officinale* Roscoe) by GC–MS. Yakugaku Zasshi (J. Pharm. Soc. Jap.) 93 (3), 318–321.

Masada, Y., Inoue, T., Hashimoto, K., Fuzioka, M., Uchino, C., 1974. Studies on the constituents of ginger (*Zingiber officinale* Roscoe) by GC–MS. Yakugaku Zasshi (J. Pharm. Soc. Jap.) 94 (6), 735–738.

Masanori, K., Kaoru, U.U., Tatsuo, H., Yutaka, H., 2002. Cell differentiation inducers and antiandrogenic active compounds from Zingiberis rhizome. Natural Medicines (Tokyo, Japan) 56 (2), 47–50.

Mustafa, T., Srivastava, K.C., Jensen, K.B., 1993. Drug Development report (9): pharmacology of ginger, *Zingiber officinale*. J. Drug Dev. 6, 25–39.

Sharma, R.K., Sarma, T.C., Leclercq, P.A., 2002. Essential oils of *Zingiber officinale* Roscoe from North East India. J. Essential Oil-bearing Plants 5 (2), 71–76.

Somepalli, V., Madabattula, R., Gottumukkala, S.V., Satyanarayana, S., 2000. Synthesis and antibacterial activity of tetrahydrocurcuminoids. Asian J. Chem. 12 (1), 141–144.

Srivas, K.C., 1984. Effects of aqueous extracts of onion, garlic and ginger on platelet aggregation and metabolism of arachidonic acid in the blood vascular system: in vitro study. Prostaglandins Leukotrienes & Medicine 13, 227–235.

Srivastava, K.C., Mustafa, T., 1992. Ginger (*Zingiber officinale*) in rheumatism and musculoskeletal disorders. Med. Hypotheses 39, 342–348.

Surh, Y.J., Lee, S.S., 1992. Enzymatic reduction of shogaol: a novel biotransformation pathway for the alpha, beta-unsaturated ketone system. Biochem. Int. 27 (1), 179–187.

Tjendraputra, E., Tran, V.H., Liu-Brennan, D., Roufogalis, B.D., Duke, C.C., 2001. Effect of ginger constituents and synthetic analogues on cyclooxygenase-2 enzyme in intact cells. Bioorganic Chem. 29, 156–163.

Wu, T.S., Wu, Y.C., Wu, P.L., Chern, C.Y., Leu, Y.L., Chan, Y.Y., 1998. Structure and synthesis of [*n*]-dehydroshogaols from *Zingiber officinale*. Phytochemistry 48 (5), 889–891.

Yu, Z., Wu, H., Ding, J., 1998. Volatile chemical components of fresh *Zingiber officinale*. Yunnan Zhiwu Yanjiu 20 (1), 113–118.